Journal of Molecular Structure 1099 (2015) 38–48

Contents lists available at ScienceDirect

Journal of Molecular Structure

journal homepage: http://www.elsevier.com/locate/molstruc

Characterization of some amino acid derivatives of benzoyl isothiocyanate: Crystal structures and theoretical prediction of their reactivity

Felix Odame [a], Eric C. Hosten [a], Richard Betz [a], Kevin Lobb [b], Zenixole R. Tshentu [a, *]

[a] Department of Chemistry, Nelson Mandela Metropolitan University, P.O. Box 77000, Port Elizabeth 6031, South Africa
[b] Department of Chemistry, Rhodes University, P.O. Box 94, Grahamstown 6140, South Africa

ARTICLE INFO

Article history:
Received 17 September 2014
Received in revised form
21 May 2015
Accepted 22 May 2015
Available online 17 June 2015

Keywords:
Benzoyl isothiocyanate
Amino acids
Crystal structures
Frontier orbitals

ABSTRACT

The reaction of benzoyl isothiocyanate with L-serine, L-proline, D-methionine and L-alanine gave 2-[(benzoylcarbamothioyl)amino]-3-hydroxypropanoic acid (**I**), 1-(benzoylcarbamothioyl)pyrrolidine-2-carboxylic acid (**II**), 2-[(benzoylcarbamothioyl)amino]-4-(methylsulfanyl)butanoic acid (**III**) and 2-[(benzoylcarbamothioyl)amino]propanoic acid (**IV**), respectively. The compounds have been characterized by IR, NMR, microanalyses and mass spectrometry. The crystal structures of all the compounds have also been discussed. Compound **II** showed rotamers in solution. DFT calculations of the frontier orbitals of the compounds have been carried out to ascertain the groups that contribute to the HOMO and LUMO, and to study their contribution to the reactivity of these compounds. The calculations indicated that the carboxylic acid group in these compounds is unreactive hence making the conversion to benzimidazoles *via* cyclization on the carboxylic acids impractical. This has been further confirmed by the reaction of compounds **I**–**IV**, respectively, with *o*-phenylene diamine which was unsuccessful but gave compound **V**.

1. Introduction

Amino acid derivatives of benzoyl isothiocyanate can be used as intermediates to construct other biologically active molecules with a thiourea backbone, and in this case the title compounds were envisaged to be converted to benzimidazoles by reacting the carboxylic acid with 1,2-diaminobenzene. The isothiocyanates can be generated by a reaction of the acylated intermediates with ammonium thiocyanate in the presence of polyethylene gylcol 400 (PEG 400) [1], and then reacted with amines to generate the thiourea derivatives. Thiourea derivatives have been synthesized through several ways. For example, ethyl isothiocyanates and aromatic amines were mixed and stirred at room temperature in acetone for 15 h to give the corresponding thioureas in high yields [2]. A simple and efficient method for the synthesis of thiourea derivatives in high purity and high yield has been reported using tetrabutyl ammonium bromide (TBAB) as a phase transfer catalyst [3]. A series of thiourea derivatives containing the quinazoline–4(3*H*) framework have been synthesized by Saeed et al. [4]. Pyrazole acyl thiourea derivatives have also been synthesized from monomethylhydrazine (or phenylhydrazine) and ethyl acetoacetate [1]. *N*-(5-Aryl-2-furonyl) thiourea derivatives containing substituted pyrimidine rings have been synthesized in good yield using PEG–400 as a phase transfer catalyst under ultrasonic irradiation [5]. Fluorinated pyrazoles, benzene sulfonylurea and thiourea derivatives as well as their cyclic sulfonylthioureas have been prepared by the reaction of brominated trifluoromethyl diketones with isocyanates and isothiocyanates [6]. Benzimidazoles conjugated to thioureas have been synthesized by the refluxing of isothiocyanates and benzimidazoles in dimethyl formamide [7].

Versatile and expeditious syntheses of taurine-derived thioureas, ureas, and guanidines using taurine isothiocyanate as the key intermediate have also been reported [8]. The thioureas were obtained by a one-pot two-step procedure starting from taurine by the isothiocyanation reaction with thiophosgene in aqueous tetrahydrofuran, followed by coupling with aliphatic and aromatic amines. Desulfurization of the thiourea derivatives with mercury(II) oxide gave either taurine-containing ureas or guanidine [8]. Urea and thiourea derivatives of diphenylphoshoramidate may be accessed by the reaction of diphenylphosphoramidate with

* Corresponding author.
E-mail address: zenixole.tshentu@nmmu.ac.za (Z.R. Tshentu).

http://dx.doi.org/10.1016/j.molstruc.2015.05.053
0022-2860/

aromatic isocyanates and isothiocyanates in tetrahydrofuran in the presence of triethylamine [9]. Multifunctional thioureas bearing a variety of functional groups at a position remote from the thiourea moiety have been synthesized *via* ruthenium catalyzed Huisgen cycloaddition [10]. The aspartic acid dimethyl ester and alanine methyl ester derivatives of benzoyl isothiocyanate have also been synthesized in acetone from the corresponding thione [11,12]. A methoxy substituted derivative of benzoyl isothiocyanate has been accessed by boiling the thione directly in methanol [13]. *N*-[Benzoylamino)thioxomethyl]amino acid derivatives have been prepared by the reaction of benzoyl isothiocyanate with various amino acids in acetone, namely, histidine, alanine, phenylalanine, serine and cysteine, however the alanine and serine derivatives were characterised by NMR only [14]. The cadmium(II) and zinc(II) complexes of the phenylalanine derivatives have also been reported and characterized by IR, NMR, and microanalysis [14]. The cobalt(II), copper(II) and nickel(II) complexes of the aspartic acid, glutamic acid, methionine, leucine and tryptophan derivatives of benzoyl isothiocyanates have been synthesized and tested for their antibacterial activity [15]. Some thiourea derivatives of various amines have also been synthesized in acetone and tested for their anti-amoebic properties [16]. Cyclohexanecarbonyl isothiocyanate has been reacted with various amines in acetone, with a slightly different work-up procedure which involved the addition of 0.1 N hydrochloric acid to the mother liquor before filtration, and this was reported to give higher yields of between 86 and 93% [17]. Benzothiazole derivatives of various carbonyl isothiocyanates have been synthesized in acetone in the presence of 3% tetrabutyl ammonium bromide (TBAB) [18].

Compounds **I**–**IV** can be useful intermediates for further synthesis of biologically relevant compounds, and in this case benzimidazole formation *via* cyclization on the amino acid carboxylic acid using polyphosphoric acid in toluene at 165 °C. It is therefore important to study their chemical properties in order to understand their reactivity since the attempted cyclization reaction was not successful but gave compound **V**. The computational studies of the frontier orbitals have been carried out and the HOMO and LUMO gaps discussed. Compounds **I**–**IV** have also been characterized by single crystal XRD. The NMR analysis (^{1}H, 1D NOESY, 2D NOESY, ^{13}C, HMBC, HSQC) of compound **II** showed the formation of rotomers in solution which was not observed in the solid state.

2. Experimental

2.1. Reagent and instrumentation

Analytical grade reagents and solvents for synthesis such as ammonium thiocyanate, L-serine, D-methionine, L-proline and L-alanine were obtained from Sigma Aldrich (USA) whilst acetone and benzoyl chloride were obtained from Merck Chemicals (SA). The chemicals were used as received (i.e. without further purification). ^{1}H NMR and ^{13}C NMR spectra were recorded on a Bruker Avance AV 400 MHz spectrometer operating at 400 MHz for ^{1}H and 100 MHz for ^{13}C using DMSO-d_6 as solvent and tetramethylsilane as internal standard. Chemical shifts are expressed in ppm. FT–IR spectra were recorded on a Bruker Platinum ATR Spectrophotometer Tensor 27. Elemental analyses were performed using a Vario Elementar Microcube ELIII. Melting points were obtained using a Stuart Lasec SMP30 whilst the masses were determined using an Agilent 7890A GC System connected to a 5975C VL–MSC with electron impact as the ionization mode and detection by a triple-Axis detector.The GC was fitted with a 30 m × 0.25 mm x 0.25 μm DB-5 capillary column. Helium was used as carrier gas at a flow rate of 1.6 mL min^{-1} with an average velocity of 30.2 cm s^{-1} and a pressure of 63.7 KPa.

2.2. General method for the synthesis of the compounds

Ammonium thiocyanate (0.10 mol, 7.6 g) was dissolved in 100 mL of acetone. Benzoyl chloride (0.10 mol, 11.3 mL) was added followed by heating under reflux at 100–120 °C for 2 h. The product was filtered and the respective amino acid was added to the filtrate and refluxed at 100–120 °C for 6 h 20 mL of water was then added and the mixture was refluxed for a further 2 h. The reaction mixture was extracted with diethyl ether, and the solvent removed *via* rotary evaporation followed by drying the compound in a high vacuum. GC–Mass spectra were recorded for the synthesized compounds and they showed molecular ion (M^+) peaks, in addition to others, which confirmed the formation the products.

2.2.1. 2-[(Benzoylcarbamothioyl)amino]-3-hydroxypropanoic acid (*I*)

The product was recrystallized and obtained as a colourless solid from acetone:water (4:1). Yield = 71%, Mp = 163–165 °C. ^{1}H NMR (ppm): 11.43 (s, N(2)–H), 11.49 (s, 1H, O(2)–H), 7.96 (d, 2H, C(12)–H, C(16)–H)), 7.65 (m, 1H, C(14)–H), 7.53 (m, 2H, C(13)–H, and C(15)–H), 5.34 (br, 1H, N(1)–H), 4.94 (t, 1H, C(3)–H), 3.88 (s, 2H, C(5)–H). ^{13}C NMR (ppm): 180.3 (C(2)–S(1), 170.7 (C(4)–O(3)), 168.3 (C(1)–(O(1)), 128.4 (C(13) and C(15)), 128.5 (C(12) and C(16)), 132.1 (C(14), 133.0C(11)), 60.5 (C(6)), 60.3 (C(3). IR (ν_{max}, cm^{-1}): 3229 (N–H), 2980 (aliphatic C–H), 1725 (C=S), 1654 (C=O), 1509 (aromatic C=C), 1164 (C–N). Anal. calcd. for $C_{11}H_{12}N_2O_4S.H_2O$: C, 46.15; H, 4.93; S, 11.20; N, 9.78. Found: C, 46.92; H, 4.87; S, 10.67; N, 9.76. LRMS (*m/z*, M^+): Found for $C_{11}H_{12}N_2O_3S$ = 268.00, Expected mass = 268.29.

2.2.2. 1-(Benzoylcarbamothioyl)pyrrolidine-2-carboxylic acid (*II*)

The product recrystallized as a white solid from acetone:water (4:1). Yield = 75%, Mp = 114–117 °C. ^{1}H NMR (ppm): 10.90 (s, 1H, O(3)–H), 7.94 (d, 1H, C(12)–H), 7.85 (d, 1H, C(16)–H), 7.58 (m, 1H, C(14)–H), 7.50 (m, 2H, C(13)–H and C(15)–H), 4.68 (t, 1H, C(21)–H)), 3.68 (m, 2H, C(24)–H), 2.02 (m,2H, C(23)–H), 1.99 (m, 2H, C(22)–H). ^{13}C NMR (ppm): 179.1 (C(2)–S(1)), 171.9 (C(3′)–O(2′)), 171.2 (C(3)–O(2)), 164.0 (C(1)–O(1)), 132.9 (C(11), 132.2 (C(14), 128.4 (C(12) and C(16)), 128.2 (C(13) and C(15)), 65.4 (C(21), 62.7 (C(24), 61.7 (C(24′), 31.0 (C(23), 29.4 (C(23′), 24.19 (C(22), 22.94 (C(22). IR (ν_{max}, cm^{-1}): 3270 (N–H), 2987 (aliphatic C–H), 1730 (C=S), 1659 (C=O), 1491 (aromatic C=C), 1182 (C–N). Anal. calcd. for $C_{13}H_{14}N_2O_3S.H_2O$: C, 52.69; H, 5.44; S, 10.83; N, 9.45. Found: C, 52.55; H, 5.64; S, 9.80; N, 9.11. LRMS (*m/z*, M^+): Found for $C_{13}H_{14}N_2O_3S$ = 278.40, Expected mass = 278.33.

2.2.3. 2-[(Benzoylcarbamothioyl)amino]-4-(methylsulfanyl) butanoic acid (*III*)

The product recrystallized as a white solid from acetone:water (4:1). Yield = 77%, Mp = 123–125 °C. ^{1}H NMR (ppm): 11.54 (s, 1H, O(2)–H), 11.28 (s,1H, N(1)–H), 7.96 (m, 2H, C(12)–H and C(16)–H), 7.65 (m, 1H, C(14)–H), 7.52 (d, 2H, C(13)–H and C(15)–H), 5.03 (1H, C(3)–H), 2.26 (m, 2H, C(7)–H), 2.17 (2H, C(5)–H), 1,99 (3H, C(6)–H). ^{13}C NMR (ppm): 180.5 (C(2)–S(1)), 171.8 (C(4)–O(3)), 168.4 (C(1)–O(1),133.1 (C(11)), 132.1 (C(14)), 128.6 (C(12) and C(16)), 128.2 (C(13) and C(15)), 66.6 (C(3)), 30.5 (C(7)), 29.2 (C(5)), 14.6 (C(6)). IR (ν_{max}, cm^{-1}): 3282 (N–H), 3202 (N–H), 2914 (aliphatic C–H), 1715 (C=S), 1664 (C=O), 1519 (aromatic C=C), 1193 (C–N) Anal. calcd. for $C_{13}H_{16}N_2O_3S_2$: C, 49.98; H, 5.16; S, 20.53; N, 8.97. Found: C, 50.40; H, 5.52; S, 20.03; N, 8.97. LRMS (*m/z*, M^+): Found for $C_{13}H_{16}N_2O_3S_2$ = 312.90, Expected mass = 312.41.

2.2.4. 2-[(Benzoylcarbamothioyl)amino]propanoic acid (*IV*)

The product recrystallized as a yellow solid from acetone:water (4:1). Yield = 65%, Mp = 161–163 °C ^{1}H NMR (ppm): 11.51 (s, 1H,

O(2)–H), 11.30 (s, 1H, N(1)–H.)), 7.93 (d, 2H, C(12)–H, and C(16)–H), 7.64 (m, 1H, C(14)–H), 7.52 (m, 2H, C(13)–H and C(15)–H), 4.85 ((q, 1H, C(3)–H), 1.49 (d, 3H, C(5)–H). ^{13}C NMR (ppm): ^{13}C NMR (ppm): 179.9 (C(2)–S(1)), 172.9 (C(4)–O(3)), 168.5 (C(1)–(O1)), 133.0C(11), 132.1C(14), 128.7 (C(12) and C(16), 128.4 (C(13) and C(15)), 63.1 (C(3)–H), 17.2C(5). IR (ν_{max}, cm^{-1}): 3384 (N–H), 2992 (aliphatic C–H), 1726 (C=S), 1678 (C=O), 1489 (aromatic C=C), 1196 (C–N). Anal. calcd. for $C_{11}H_{12}N_2O_3S$: C, 52.37; H 4.79; S 12.71; N 11.10. Found: C, 52.59; H 5.11; S 12.56 N; 11.07. LRMS (*m/z*, M$^+$): Found for $C_{11}H_{12}N_2O_3S$ = 252.00, Expected mass = 252.29.

2.2.5. 2-Phenyl-1H-benzimidazole (**V**)

15 g of polyphosphoric acid, in 5 mL of toluene, was heated at 120 °C for 30 min. Compounds **I**, **II**, **III** and **IV** (0.20 mol) and *o*-phenylenediamine (0.2 mol) were added and the mixture was heated at 165 °C for 6 h. After cooling, 20 mL of water was added with stirring and then sodium hydrogen carbonate was added until effervescence ceased. The dark brown precipitate obtained was re-dissolved in little methanol and placed on the silica gel column and eluted with methanol:ethyl acetate (1:1). The product was recrystallized from ethanol:toluene (1:1) and obtained as a brown solid. Yield = 55–68%, Mp = 240–242 °C. ^{1}H NMR (ppm): 8.20 (m, 2H), 7.61 (m, 2H), 7.56 (m, 2H), 7.48 (m, 1H), 7.21 (m, 2H), ^{13}C NMR (ppm): 151.2 (C=N), 130.0 (Ph–H), 129.9 (Ph–H), 128.9 (Ph–H), 126.4 (Ph–H), 122.1 (Ph–H), IR (ν_{max}, cm^{-1}): 3048 (N–H), 2961 (C–H), 2850 (C–H), 1539 (C=N), 1461 (C=C), 1443 (C–N). Anal. Calcd for $C_{13}H_{10}N_2$: C, 80.39; H, 5.19; N, 14.42. Found: C, 80.29; H, 5.32; N, 14.64. Found for $C_{13}H_{10}N_2$ = 194.10, Expected mass = 194.23.

2.3. X-ray crystallography

X-ray diffraction analyses of **I**–**IV** were performed at 200 K using a Bruker Kappa Apex II diffractometer with monochromated MoKα radiation (λ = 0.71073 Å). APEXII [19] was used for data collection and SAINT [19] for cell refinement and data reduction. The structures were solved by direct methods using SHELXS-2013 [20] and refined by least-squares procedures using SHELXL-2013 [20] with SHELXLE [21] as the graphical interface. All non-hydrogen atoms were refined anisotropically. Carbon-bound H atoms were placed in calculated positions (C–H 0.95 Å for aromatic carbon atoms and C–H 0.99 Å for methylene groups) and were included in the refinement in the riding model approximation, with U_{iso}(H) set to 1.2U_{eq}(C). The H atoms of the methyl groups were allowed to rotate with a fixed angle around the C–C bond to best fit the experimental electron density (HFIX 137 in the SHELX program suite [19]), with U_{iso}(H) set to 1.5U_{eq}(C). The H atom of the hydroxyl group was allowed to rotate with a fixed angle around the C–O bond to best fit the experimental electron density (HFIX 147 in the SHELX program suite [20]), with U_{iso}(H) set to 1.5U_{eq}(O). Nitrogen-bound H atoms were located on a difference Fourier map and refined freely. Data were corrected for absorption effects using the numerical method implemented in SADABS [19].

2.4. Computational studies

The calculations were carried out using Gaussian 09 program. Molecular geometries of the singlet ground state of all the compounds were fully optimised in the gas phase at the density functional theory (DFT) level of theory using B3LYP/6-31++G. For each compound a frequency calculation was carried out to ensure that the optimized molecular structure corresponded to a minimum, thus only positive frequencies were expected. The structures were generated using Chemcraft.

3. Results and discussion

3.1. Synthesis and characterization

The syntheses of compounds **I**, **III** and **IV** were readily achieved by the reaction of benzoyl isothiocyanate with the different amino acids (Scheme 1). Scheme 2 gives the reaction path for compound **II**. The lone pair of electrons on the nitrogen atom of the amino acid attacks the carbon of the thione. This shifts the electron density onto the nitrogen of the isothiocyanate allowing it to abstract a proton from the amine of the amino acid. The FTIR, ^{1}H NMR and ^{13}C NMR confirmed the formation of the amino acid derivatives. Compound **V** (Schemes 1 and 2) was accessed by the reaction of compounds **I**–**IV**, respectively, with *o*-phenylene diamine with the diamine attacking the carbonyl close to the benzene ring (benzoyl group) instead of the carboxylic acid to form **VI**.

The FTIR spectra for compounds **I**–**V** are provided in Figs. S1–S5 in the Supplementary Information. The ^{1}H NMR spectra for compounds **1**–**V** and ^{13}C NMR spectra for compounds **1**, **III**, **1V** and **V** are also provided in Figs. S6–S15 in the Supplementary Information. The nitrogen protons which do not appear in the ^{1}H NMR spectra of compounds **II**, **III** and **IV** exchange with the residual water molecules in DMSO hence are undetectable. The ^{13}C NMR spectrum of compound **II** (Fig. 1) showed six methylene groups instead of three which occurred at 54.33, 51.72, 30.96, 29.44, 24.19, and 22.94. This was also confirmed in the DEPT spectrum (Fig. 2). This showed that compound **II** possibly exists as two rotamers in solution. Fig. S16 gives the ^{1}H–^{1}H COSY for compound **I**. Figs. S17–S19 present the ^{1}H–^{1}H COSY, 1D NOESY and HMBC spectra of compound **II**, and they showed further evidence of formation of rotamers. The two rotamers in solution are formed by restricted rotation around the nitrogen of the proline, specifically around the N(2)-C(2) bond, making the carbon signals for all the four carbon atoms in the proline ring double. This also gives rise to two carbonyl signals for the proline part of compound **II** as evident in the CNMR spectrum. The 2D NOESY spectrum (Fig. 3) showed an exchange between the signals at 4.42 and 4.62 ppm, and both signals are attached to the same carbon that changes position as indicated in the HSQC spectrum (Fig. 4).

3.2. Crystal structures

Compounds **I**, **II** and **III** were recrystallized from acetone:water (4:1) as colourless crystals, whilst compound **IV** was recrystallized from acetone:water (4:1) as yellow crystals. The crystallographic data, selected bond lengths, bond angles and torsion angles for the structures of **I**–**IV** are provided in Tables 1 and 2. Compounds **I** and **II** crystallized in orthorhomic space group $P2_12_12_1$, whilst compound **III** crystallized in monoclinic space group $P2_1$ and compound **IV** in orthorhomic space group $C2_22_1$. The absence of rotamers in the solid state was confimed during the refinement procedure by means of the Flack parameter in each case.

The ORTEP diagram of compound **I** is presented in Fig. 5. The experimental bond distance of S(1)–C(2) = 1.670(2) Å in compound **I** is consistent with the C=S of the thione [22], whilst the C(1)–O(1) and C(4)–O(3) bond distances of 1.233(2) Å and 1.202(2) Å show the presence of the carbonyl bond of the amide and the carbonyl of the carboxylic acid, respectively. The bond distance of C(1)–N(1) = 1.372(2) Å is indicative of the C–N bond of the amide. The O(2)–C(4)–O(3) bond angle of 124.8(2)° is consistent with the bond angle around the sp^2 carbon of the carboxylic acid whilst the S(1)–C(2)–N(2) bond angle of 125.2(1)° indicated the presence of the sp^2 carbon of the thione. The O(1)–C(1)–N(1) bond angle of 121.6(1)° also showed the presence of the sp^2 carbon of the amide. The C(2)–N(1)–C(1)–O(1) torsion angle of 6.1(2)° confirmed the

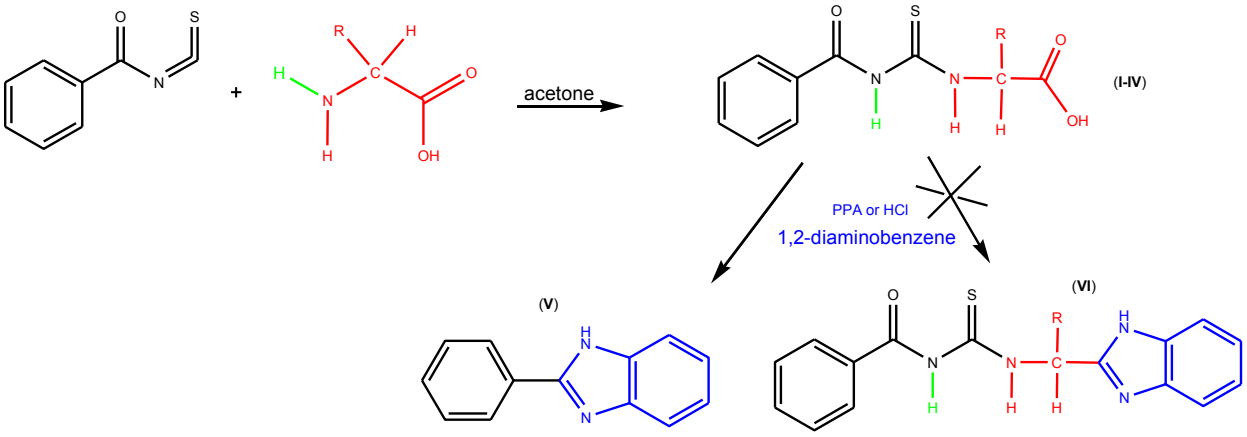

Scheme 1. Synthesis scheme for compounds **I** and **III**–**V**.

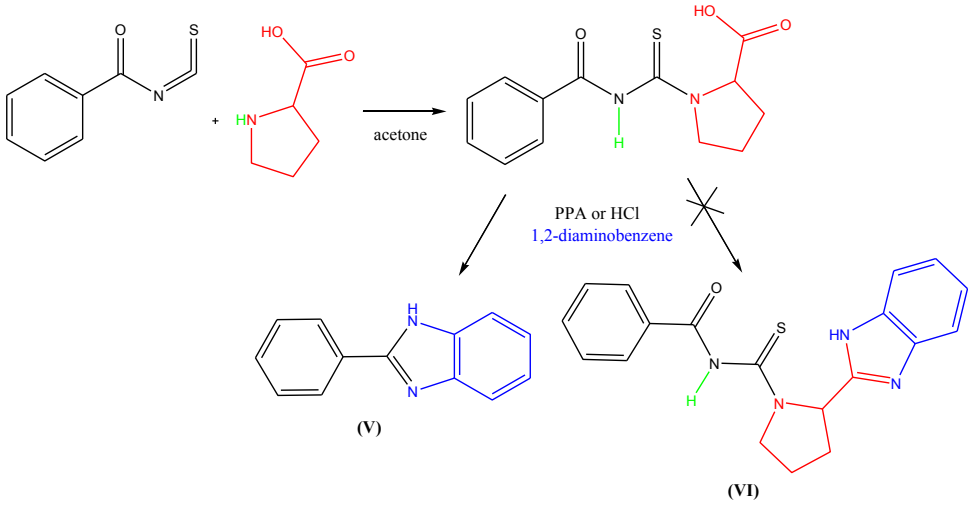

Scheme 2. Synthesis scheme for compounds **II** and **V**.

rigidity around the carbonyl of the amide whilst the C(3)–N(2)–C(2)–S(1) torsion angle of −7.3(2)° confirmed the rigidity around the thione.

There is an intramolecular hydrogen bond between the carbonyl of the amide O(1) and the nitrogen from the amino acid N(2) (Fig. S18). The carbonyl (O(1)) also forms an intermolecular hydrogen bond with the hydroxyl group O(4) of the adjoining molecule which also forms a bond with the water molecule. The

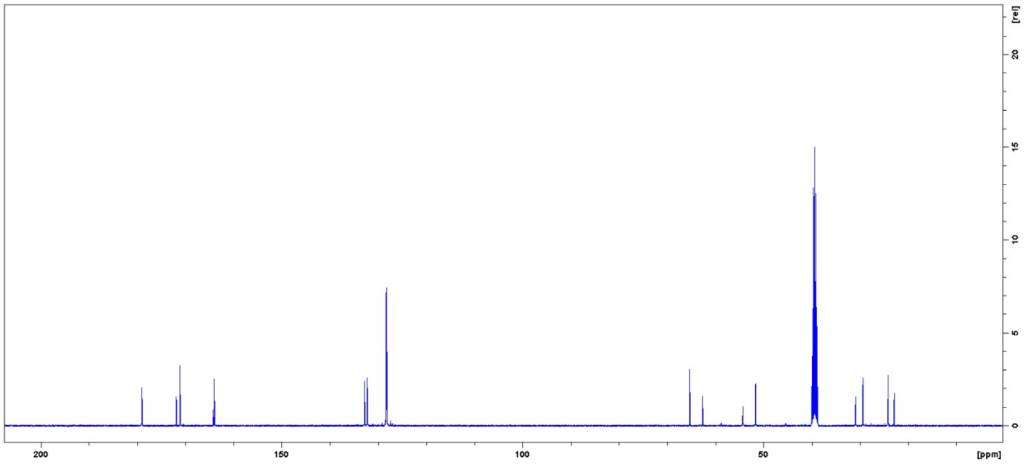

Fig. 1. ^{13}C NMR spectrum of compound **II**.

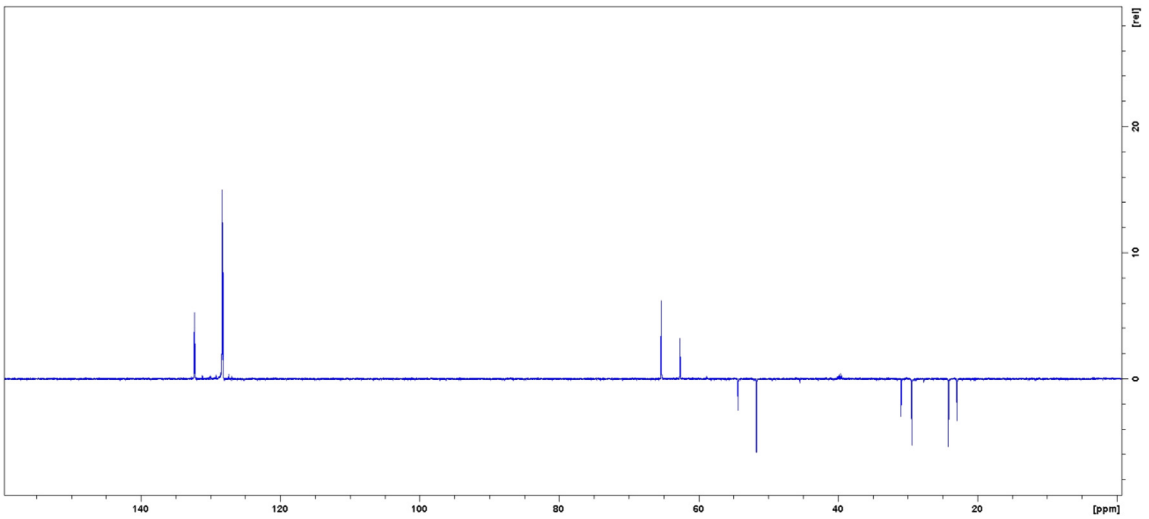

Fig. 2. DEPT spectrum of compound **II**.

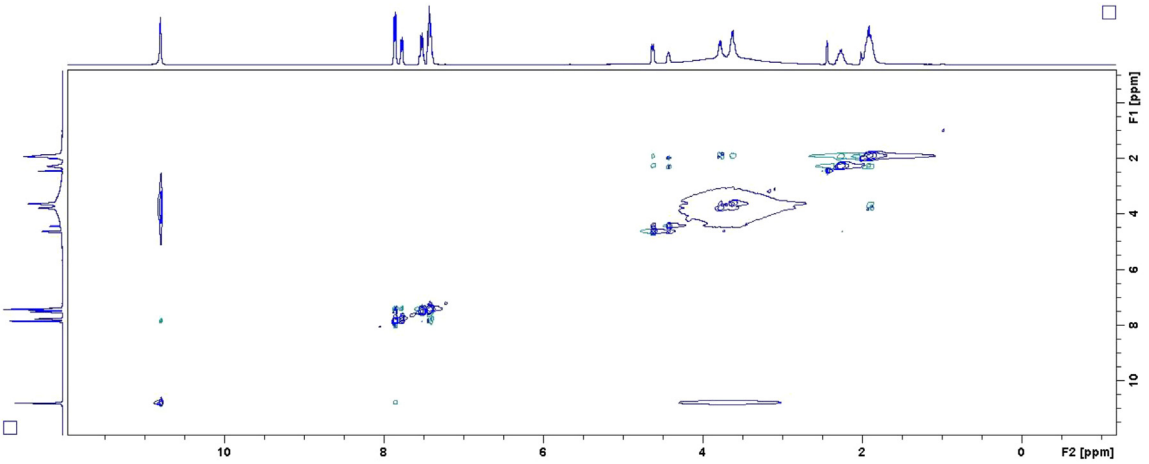

Fig. 3. 2D NOESY spectrum of compound **II**.

thione S(1) also forms a bond with a water molecule. The packing of compound **I** showed the presence of four molecules in the unit cell (Fig. S19).

The structure of compound **II** is presented in Fig. 6. The bond distances of O(2)–C(3) and C(1)–O(1) which were 1.201(2) Å and 1.229(2) Å are consistent with the carbonyl of the carboxylic acid

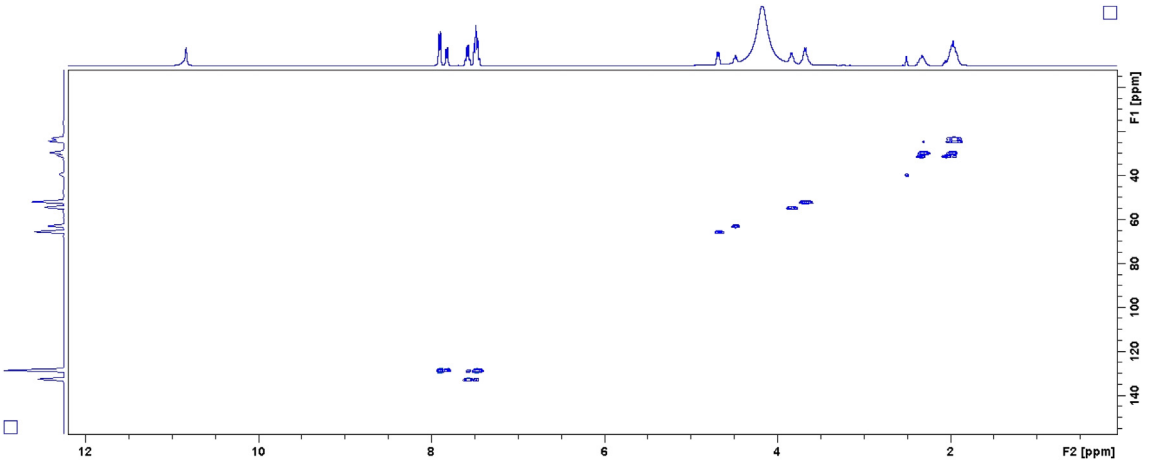

Fig. 4. HSQC spectrum of compound **II**.

Table 1
Crystallographic data and structure refinement summary for compounds **I**–**IV**.

Property	Compound **I**	Compound **II**	Compound **III**	Compound **IV**
CCDC number	1014079	1014083	1014284	1014322
Empirical formula	$C_{11}H_{12}N_2O_4S,H_2O$	$C_{13}H_{14}N_2O_3S,H_2O$	$C_{13}H_{16}N_2O_3S_2$	$C_{11}H_{12}N_2O_3S$
Formula weight	286.31	296.35	312.42	252.30
Crystal system	Orthorhombic	Orthorhombic	Monoclinic	Orthorhombic
Space group	$P2_12_12_1$	$P2_12_12_1$	$P2_1$	$C2_22_1$
a (Å)	7.0613(3)	8.8347(5)	5.1663(2)	8.2584(3)
b (Å)	11.0752(4)	11.8182(7)	1.4170(5)	21.7331(8)
c (Å)	16.5713(7)	13.3896(8)	12.7108(5)	13.4905(6)
α (°)	90	90	90	90
β (°)	90	90	96.843(1)	90
γ (°)	90	90	90	90
V [Å^3]	1295.96(9)	1398.01(14)	744.39(5)	2421.28(17)
Z	4	4	2	8
D(calc) (g/cm^3)	1.467	1.408	1.394	1.384
μ(MoKa) (/mm)	0.268	0.246	0.365	0.265
F(000)	600	624	328	1056
Crystal size (mm)	0.26 × 0.39 × 0 0.52	0.47 × 0.48 × 0.56	0.16 × 0.37 × 0.49	0.23 × 0.53 × 0.72
Temperature (K)	200	200	200	200
Radiation (Å)	0.71073	0.71073	0.71073	0.71073
θ Min–Max (°)	2.2–28.3	2.8–28.4	2.4–28.3	1.9–28.3
Dataset	−7:9; −14:9; −22:20	−1:8; −15:13; −17:17	−6:4; −14:15; −16:16	−11:9; −25:28; −15:17
Tot., Uniq. Data	6893, 3088	10872, 3334	6845, 3344	6792, 3009
R_{int}	0.010	0.014	0.017	0.014
[I > 2.0 sigma(I)]	2991	3224	3176	2879
Nref, Npar	3088,180	3334, 195	3344,185	3009, 164
R	0.0227	0.0240	0.0252	0.0238
$_wR_2$	0.0643	0.0650	0.0654	0.0659
S	1.09	1.03	1.03	1.04
Max. and Av. shift/error	0.00, 0.00	0.00, 0.00	0.000,0.00	0.000,0.00
Min. residual. density. [e/Å^3]	−0.17	−0.17	−0.20	−0.14
Max. residual. density. [e/Å^3	025	0.24	0.26	0.25
Flack parameter	0.020(13)	0.002(14)	0.00(2)	0.012(19)

Table 2
Selected bond length (Å), bond angles and torsion angles of compounds **I**–**IV**.

Bond lengths	**I**	**II**	**III**	**IV**
	Expt	Expt	Expt	Expt
S(1)–C(2)	1.670(2)	1.661(2)	1.676(2)	1.677(1)
O(1)–C(1)	1.232(2)	1.229(2)	1.226(2)	1.222(2)
N(1)–C(2)	1.399(2)	1.420(2)	1.385(3)	1.323(2)
N(1)–C(1)	1.372(2)	1.367(2)	1.383(3)	1.386(2)
N(2)–C(2)	1.331(2)	1.326(2)	1.331(3)	1.487(2)
C(1)–C(11)	1.489(2)	1.488(2)	1.486(3)	1.487(2)
S(2)–C(7)	-	-	1.793(3)	-
S(2)–C(6)	-	-	1.801(2)	-
Bond angles	**I**	**II**	**III**	**IV**
O(1)–C(1)–N(1)	121.8(1)	121.8(1)	121.5(2)	122.0(1)
O(1)–C(1)–C(11)	121.6(1)	120.9(1)	121.3(2)	121.8(1)
S(1)–C(2)–N(1)	118.3(1)	119.2(1)	120.9(2)	119.6(1)
S(1)–C(2)–N(2)	125.2(1)	124.4(1)	122.3(2)	123.5(1)
N(1)–C(1)–C(11)	116.6(1)	117.3(1)	117.2(2)	116.2(1)
N(1)–C(2)–N(2)	116.6(1)	116.3(1)	116.8(2)	116.8(1)
C(1)–N(1)–C(2)	127.8(1)	123.2(1)	126.9(2)	127.4(1)
Torsion angles	**I**	**II**	**III**	**IV**
N(1)–C(1)–C(11)–C(16)	−158.7(2)	−21.1(2)	−174.2(2)	−15.8(3)
C(2)–N(1)–C(1)–O(1)	6.1(2)	7.1(2)	3.5(3)	−6.0(3)
C(1)–N(1)–C(2)–S(1)	176.0(1)	121.5(1)	179.2(2)	179.3(1)
C(3)–N(2)–C(2)–S(1)	−7.3(2)	-	6.1(3)	2.8(2)
O(1)–C(1)–C(11)–C(16)	1.0(2)	159.2(2)	6.7(3)	162.7(2)
C(1)–N(1)–C(2)–N(2)	−3.2(2)	−60.3(2)	0.4(3)	−0.4(2)
O(1)–C(1)–C(11)–C(12)	−156.7(2)	−20.2(2)	−173.4(2)	−14.4(3)

and the carbonyl of the amide, respectively. This also compared favourably with the carbonyl bond distances in compound **I**. The bond distance of C(1)–N(1) = 1.367(2) Å indicated the C–N bond of the amide and it was comparable to the C–N bond distance in

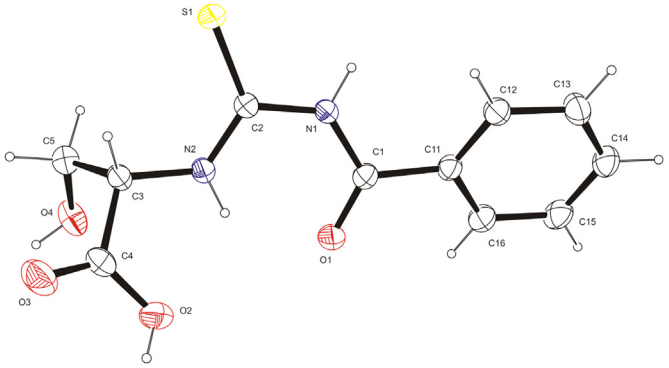

Fig. 5. An ORTEP view of compound **I** showing 50% probability displacement ellipsoids and the atom labelling.

compound **I** which was 1.372(2) Å. The bond distance of S(1)–C(2) = 1.661(2) Å showed the presence of the C=S of the thione and was comparable to that of compound **I** (1.670(2) Å). The O(3)–C(3)–O(2) bond angle of 125.0(1)° is indicative of the sp^2 carbon of the carbonyl of the carboxylic acid and the N(1)–C(1)–O(1) bond angle of 121.8(1)° also confirmed the presence of the sp^2 carbon of the carbonyl and these were comparable to the bond angles observed in compound **I**. The S(1)–C(2)–N(1) bond angle of 119.2(1)° also indicated the presence of the sp^2 carbon of the thione. The C(2)–N(1)–C(1)–O(1) torsion angle of 7.1(2)° was consistent with the rigidity in the amide whilst the C(21)–N(2)–C(2)–S(1) torsion angle of 1.3(2)° confirmed the rigidity around the thione. There exists an intermolecular hydrogen bond in compound **II** between the carbonyl of the amide O(1) and a water molecule which is also bonded to the carbonyl O(2) of the carboxylic acid of

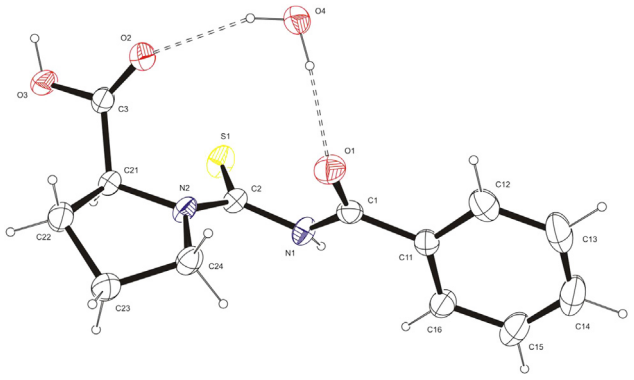

Fig. 6. An ORTEP view of compound **II** showing 50% probability displacement ellipsoids and the atom labelling.

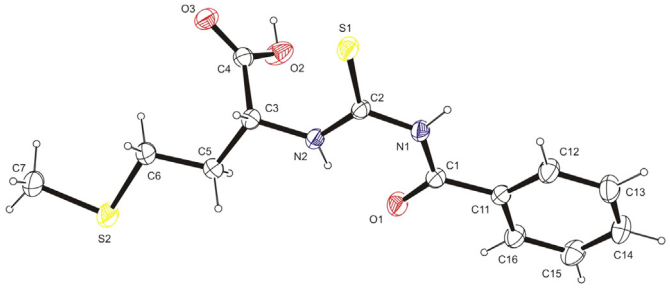

Fig. 7. An ORTEP view of compound **III** showing 50% probability displacement ellipsoids and the atom labelling.

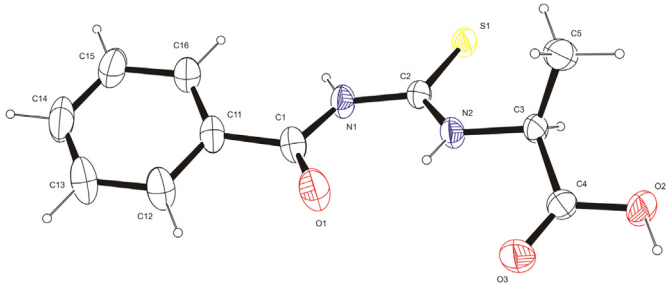

Fig. 8. An ORTEP view of compound **IV** showing 50% probability displacement ellipsoids and the atom labelling.

the same molecule and the hydroxyl O(3) of the adjoining molecule (Fig. S20). The packing of the molecules of compound **II** in a unit cell shows four molecules in each unit cell (Fig. S21).

The ORTEP diagram of compound **III** is presented in Fig. 7. The bond lengths and angles as well as tosion angles compared well with those of compounds **I** and **II** (Table 2). There is an intramolecular bond between the carbonyl O(1) of the amide and the nitrogen N(2) from the amino acid. There exists an intermolecular hydrogen bond in compound **III** between the thione S(1) and the hydroxyl O(2) of the adjoining molecule and also between the nitrogen N(1) of the amide and the carbonyl O(3) of the carboxylic acid of the adjoining molecule (Fig. S22). The packing of compound **III** shows two molecules in the unit cell (Fig. S23).

The ORTEP diagram of compound **IV** is presented in Fig. 8. The bond distances and angles as well as the torsion angles were comparable with those of compounds **I-III** (Table 2). There is an intramolecular hydrogen bond in compound **IV** between the carbonyl O(1) of the amide and the nitrogen N(2) from the amino acid (Fig. S24). There also exists an intermolecular bond between the thione S(1) and the hydroxyl O(2) of the adjoining molecule. The packing of the molecules of compound **IV** in a unit cell shows eight molecules in each unit cell (Fig. S25).

3.3. HOMO-LUMO analysis

In view of the fact that compounds **I**–**IV** are useful intermediates in accessing other complex molecules, it was important to carry out some theoretical studies to characterise the nature of these compounds in terms of chemical reactivity. In fact, a chemical reaction that was attempted on compounds **I**–**IV**, i.e. a cyclization reaction with 1,2-diaminobenzene at the carboxylic acid site to form benzimidazoles, has been unsuccessful yielding rather a benzimidazole through the diamine attacking the carbonyl of the benzoyl group (compound **V**) instead of the carboxylic acid site. This prompted us to carry out some computational studies in order to predict the reactivity of these compounds. The highest occupied molecular orbital and lowest unoccupied molecular orbital energy separations, HOMO–LUMO energy gaps, have been evaluated by DFT methods. The frontier orbitals are useful in predicting the most reactive position in π-electron systems [23] and to explain several types of reactions in a conjugated system like benzoyl isothiocyanate.

Benzoyl isothiocyanate is characterised by a small highest occupied molecular orbital-lowest unoccupied molecular orbital (HOMO–LUMO) separation, which is the result of a significant degree of intramolecular charge transfer from the end capping electron-donor groups through a π-conjugated path [24]. The HOMO and LUMO are the main orbitals that determine chemical stability of the species [25]. The HOMO, which represents the ability to donate an electron, is delocalised over the entire molecule except the carbonyl and carbon of the thione whilst the LUMO (which represent the ability to accept an electron) shows delocalization of it orbitals over both the carbon atoms of the carbonyl and the thione indicating that both are susceptible to attack by an incoming group but because the carbonyl is sterically hindered the carbon of the thione is the preferred site of attack and this attack is

Table 3
Summary of the HOMO-LUMO energies for compounds **I**–**IV** and the starting materials.

	HOMO (kJ/mol)	LUMO (kJ/mol)	HOMO–LUMO gap (kJ/mol)
Benzoyl isothiocyanate	−715.16	−498.40	216.76
Compound **I**	−675.93	−243.75	432.18
Serine	−692.24	−85.64	606.60
Compound **II**	−616.00	−205.55	410.45
Proline	−638.97	−74.83	564.14
Compound **III**	−564.17	−214.50	349.67
Methionine	−599.43	−91.34	508.09
Compound **IV**	−651.52	−233.12	418.40
Alanine	−678.72	−86.35	592.37

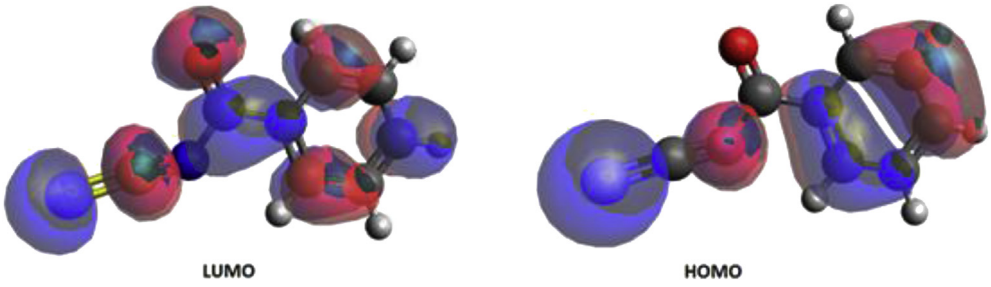

Fig. 9. The atomic orbitals compositions of the frontier molecular orbitals for benzoyl isothiocyanate.

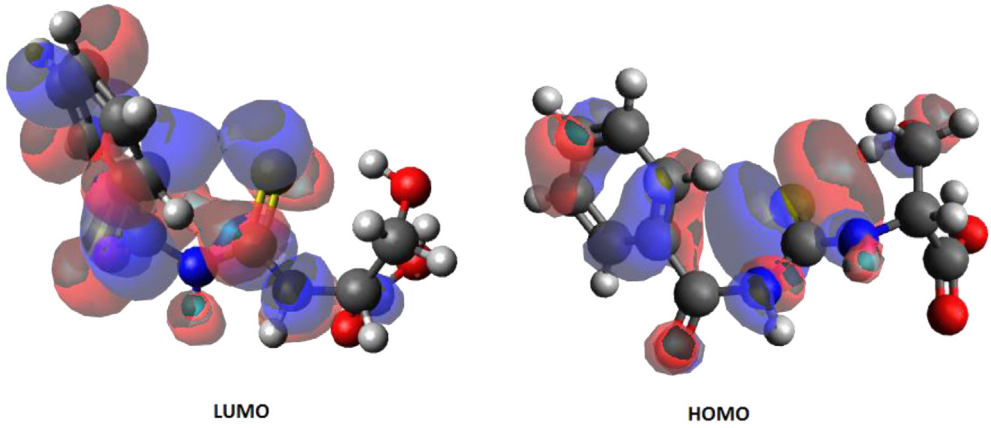

Fig. 10. The atomic orbitals compositions of the frontier molecular orbital for compound **I**.

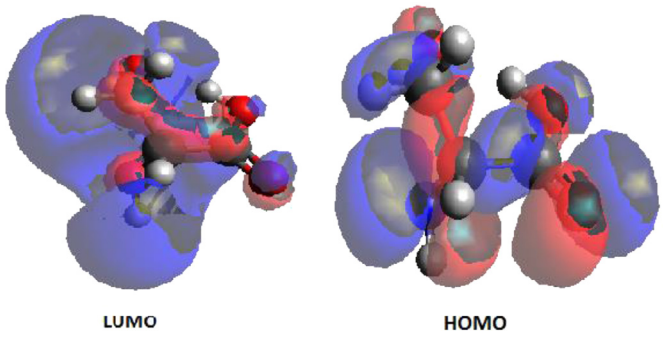

Fig. 11. The atomic orbitals compositions of the frontier molecular orbital for serine.

further stabilized by charge transfer through the benzene ring. The energy of the HOMO is directly related to the ionization potential whilst the energy of the LUMO is related to the electron affinity. The energy difference between HOMO and LUMO orbitals, known as the energy gap, determines the stability or reactivity of molecules [26]. A narrow energy gap for benzoyl isothiocyanate is consistent with its high reactivity. The energy gap is a critical parameter in determining molecular electrical transport properties because it is a measure of electron conductivity [27]. The hardness of a molecule also corresponds to the gap between the HOMO–LUMO orbitals [28]. Large HOMO–LUMO gap indicates high stability and resistance to charge transfer, therefore, hard molecules have a large HOMO–LUMO gap.

Table 3 gives the computed energy gap between the LUMO and HOMO of compounds **I**–**IV** and benzoyl isothiocyanate as well as

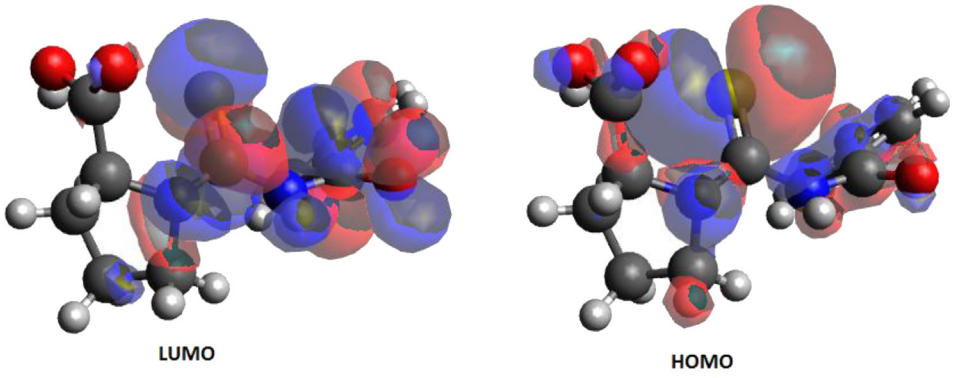

Fig. 12. The atomic orbitals compositions of the frontier molecular orbitals for compound **II**.

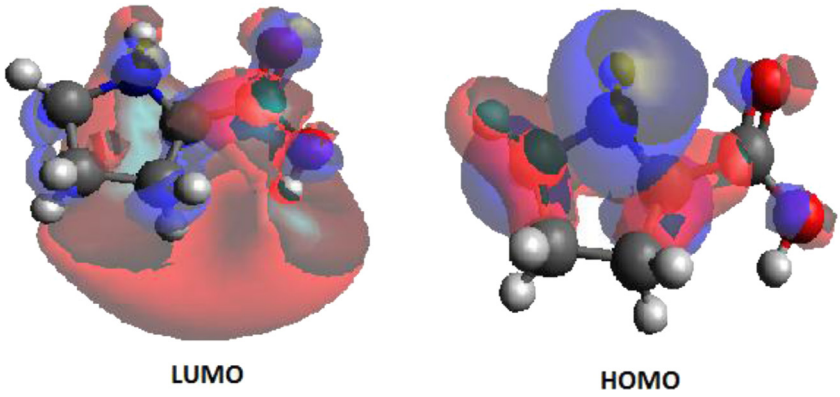

Fig. 13. The atomic orbitals compositions of the frontier molecular orbitals for proline.

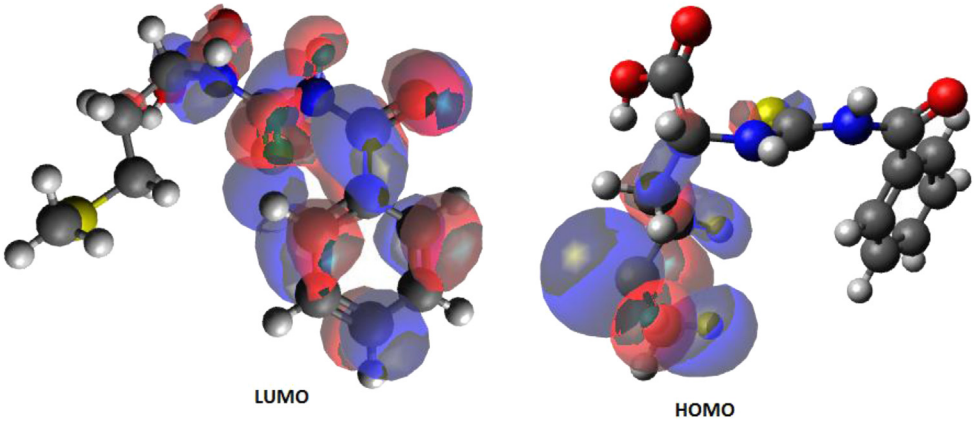

Fig. 14. The atomic orbitals compositions of the frontier molecular orbitals for compound **III**.

the amino acids. The computed energy gap between the LUMO and HOMO of benzoyl isothiocyanate is narrow which implies that it is a soft molecule [29]. Compound **I** with a HOMO–LUMO gap of 432.18 kJ/mol is lower compared to that of serine which is 606.60 kJ/mol, confirming that L-serine is harder and less reactive than compound **I**, even though their sites of reactivity differ. L-Proline with a HOMO–LUMO gap of 564.14 kJ/mol is harder but less reactive than compared **II** which has a HOMO–LUMO gap of 410.45 kJ/mol, but the reactivity of these compounds are concentrated on different sites of the molecules. Compound **III** with a HOMO–LUMO gap of 349.67 kJ/mol is harder but less reactive than D-methionine which has a HOMO–LUMO gap of 508.09 kJ/mol, and alanine with a HOMO–LUMO gap of 592.37 kJ/mol is hard and less receive than compound **IV** which is 418.40 kJ/mol. From this information, it is not clear why the carboxylic acid site is less reactive in the benzoyl isothiocyanates derivatives compared with the amino acids since these molecules are must softer than the parent amino acids. This prompted the study of the frontier orbitals.

Fig. 9 shows the HOMO and LUMO orbitals of benzoyl isothiocyanate. The HOMO is delocalised over the thione, nitrogen and the ring with the oxygen atom making no contribution. whilst the LUMO is delocalised over nearly the entire molecule. This suggests that the entire molecule is involved in the acceptance of electrons which makes this species very reactive.

The frontier orbitals of compound **I** (Fig. 10) shows that the HOMO is mostly concentrated on the sulfur of the thione, the

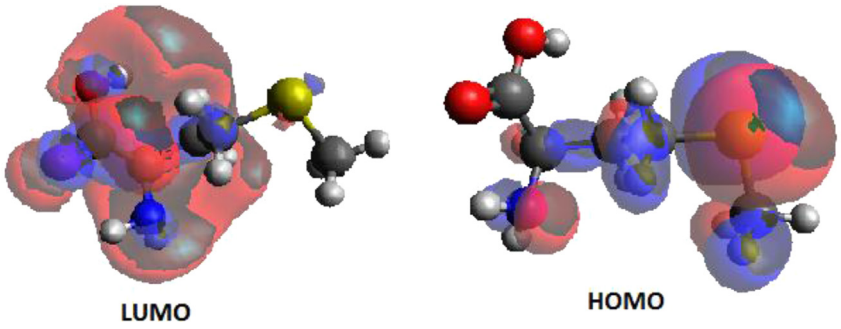

Fig. 15. The atomic orbitals compositions of the frontier molecular orbitals for methionine.

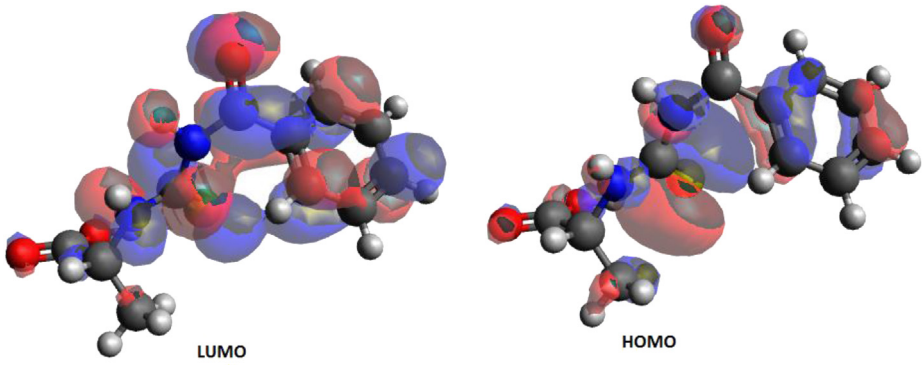

Fig. 16. The atomic orbitals compositions of the frontier molecular orbitals for compound **IV**.

nitrogen atoms and the phenyl ring, whilst the LUMO is largely delocalised over the thione, the nitrogen atoms, the carbonyl and over the benzene ring which aids in stabilising the compound during charge transfer *via* delocalization over the benzene ring. The carboxylic acid has no contribution to the frontier orbitals (LUMO) hence is unreactive in the compound. This further confirmed the inability to convert it to a benzimidazole by reacting it with 1,2-diaminobenzene. The frontier orbitals of serine (Fig. 11) are distributed over the entire molecule with most of the atoms making a contribution. The carboxylic acid makes a little contribution to the LUMO hence the cyclization should be possible on a free serine.

The frontier orbitals of compound **II** are shown in Fig. 12. The HOMO is mostly concentrated on the sulfur of the thione and is slightly delocalised on the nitrogen atoms whilst the LUMO is largely delocalised over the entire molecule except the carboxylic the acid and the methylene groups. Once again, the carboxylic acid was unreactive because it makes no contribution to the frontier orbitals which confirmed why it could not be converted to a benzimidazole. The frontier orbitals of proline are delocalized over nearly the entire molecule in LUMO confirming the possibility for benzimidazole formation whilst in the HOMO the orbital is delocalized over the nitrogen and the surrounding carbon atoms (Fig. 13).

Fig. 14 shows the frontier orbitals of compound **III**. The HOMO is mostly concentrated on the sulfur atoms and the methylene groups from the methionine whilst the LUMO is mostly delocalised over the benzene ring, the carbonyl, the nitrogen atoms and the thione. The delocalisation of the LUMO over the benzene ring aids in stabilising the compound during charge transfer. The carboxylic acid makes no contribution to the frontier orbitals (LUMO) which again confirmed its unreactivity. In frontier orbitals of methionine (Fig. 15) the LUMO is delocalised over the entire molecule except the sulfur and methyl group attached to it, whilst its HOMO is delocalized on the entire molecule except the carboxylic acid.

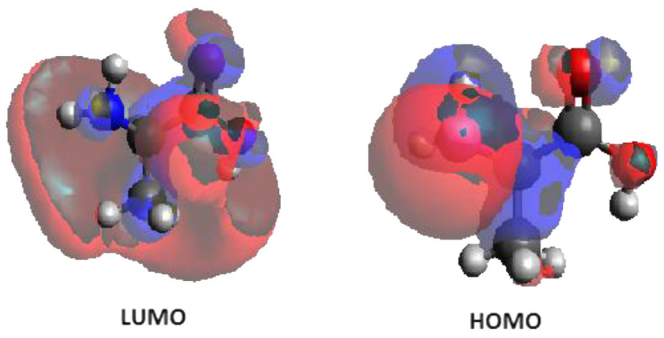

Fig. 17. The atomic orbitals compositions of the frontier molecular orbitals for alanine.

The frontier orbitals of compound **IV** are shown in Fig. 16. The HOMO is mostly concentrated on the sulfur of the thione and is slightly delocalised on the nitrogen and the carboxylic acid whilst the LUMO is largely delocalised over the entire molecule except the carboxylic acid and the methyl group. The carboxylic acid could not be functionalized to a benzimidazole by the attachment of 1,2-diamonobenzene due to the fact that the carboxylic acid has no contribution to the LUMO, which would receive the incoming electrons. The frontier orbitals of alanine in Fig. 17 shows delocalization over the entire molecule in the LUMO whilst the HOMO is also delocalized over the entire molecule with little contribution from the carboxylic acid.

The cyclization to form a benzimidazole using the alanine has been reported to be accessed by solvent free melting [30] and also in the presence of a mixture of orthophosphic acid and polyphosporic acid *via* microwave irradiation [31]. Hence, the compounds were not reproduced here. However, the theoretical calculations indicate that the amino acid derivatives of benzoyl isothiocyanate are not reactive to the cyclization reaction with 1,2-diaminobenzene at the carboxylic acid site (Scheme 1).

4. Conclusions

2-[(Benzoylcarbamothioyl)amino]-3-hydroxypropanoic acid (**I**), 1-(benzoylcarbamothioyl)pyrrolidine-2-carboxylic acid (**II**), 2-[(benzoylcarbamothioyl)amino]-4-(methylsulfanyl)butanoic acid (**III**), and 2-[(benzoylcarbamothioyl)amino]propanoic acid (**IV**) have been synthesized from the reaction of L-serine, L-proline, D-methionine and L-alanine with benzoyl isothiocyanate, respectively. The compounds have been characterized by IR, NMR, microanalyses and mass spectrometry. The crystal structures of all the compounds have also been discussed. Compound **II** exhibited rotamers in solution. DFT calculations of the frontier orbitals showed that the carboxylic acid group in these compounds was unreactive which confirmed the unsuccessful attempts to convert these compounds to benzimidazoles *via* cyclization with 1,2-diaminobenzene.

Acknowledgements

The authors are grateful to the Medical Research Council (MRC) of South Africa for financial assistance and Felix Odame would also like to thank the Faculty of Science (NMMU) for awarding him a bursary for his studies (2013 and 2014). The NMMU RCD is also acknowledged by Felix Odame for the bursary funding (PGRS) for 2015. We would also like to express our gratitude to the Centre for

High Performance Computing (CHPC) in Cape Town for the use of their modelling resources.

Appendix A. Supplementary data

Supplementary data related to this article can be found at http://dx.doi.org/10.1016/j.molstruc.2015.05.053.

References

[1] J. Wu, Q. Shi, Z. Chen, M. He, L. Jin, D. Hu, Molecules 17 (2012) 5139–5150.
[2] A. Yahyazadeh, Z. Ghasemi, Eur. Chem. Bull. 2 (2013) 573–575.
[3] S. Saeed, N. Rashid, M. Ali, R. Hussain, P. Jones, Eur. J. Chem. 1 (2010) 221–227.
[4] S. Saeed, R. Hussain, Eur. Chem. Bull. 2 (2013) 465–467.
[5] S.J. Xue, S.Y. Ke, T.B. Wei, J. Chin. Chem. Soc. 51 (2004) 1013–1018.
[6] H.M. Fadallah, K.A. Khan, A.M. Asir, J. Fluor. Chem. 132 (2011) 131–137.
[7] G.W. Lee, N. Singh, D.O. Jang, Tetrahedron Lett. 490 (2008) 1952–1956.
[8] J.M. Marquez, O. Lopez, I. Maya, J. Fuentes, J.G. Fernandez-Bolanos, Tetrahedron Lett. 49 (2008) 3912–3915.
[9] G. Madhava, V.K. Subbaiah, R. Srenivasulu, C.N. Raju, Der Pharm. Lett. 4 (2012) 1194–1201.
[10] K. Takasu, T. Azuma, I. Enkhtaivan, Y. Takemoto, Molecules 15 (2010) 8327–8348.
[11] F. Odame, E. Hosten, Z.R. Tshentu, R. Betz, Z. Kristallogr. NCS 229 (2014) 337–338.
[12] F. Odame, E. Hosten, Z.R. Tshentu, R. Betz, Z. Kristallogr. NCS 230 (2015) 9–10.
[13] F. Odame, E. Hosten, Z.R. Tshentu, R. Betz, Z. Kristallogr. NCS 229 (2014) 329–330.
[14] A.T. Kabbani, H. Ramadam, H.H. Hammud, A.M. Ghannoum, JUCTM 40 (2005) 339–344.
[15] D.M.H. AL-Mudhaffar, D.S. Al-Edani, S.M. Dawood, J. Korean Chem. Soc. 54 (2010) 506–514.
[16] M.A. Ibrahim, M.S.M. Yusof, N.M. Amin, Molecules 19 (2014) 5191–5204.
[17] C.K. Özer, H. Arslan, D. VanDerveer, N. Külcü, Molecules 14 (2009) 655–666.
[18] A.G. Patel, K.N. Raval, S.P. Patel, K.S. Patel, S.V. Patel, J. Pharma Res. 4 (2012) 1–4.
[19] APEX2, SADABS and SAINT. Bruker AXS Inc., Madison, WI, USA, 2010.
[20] G.M. Sheldrick, Acta Cryst. A 64 (2008) 112–122.
[21] C.B. Hübschle, G.M. Sheldrick, B. Dittrich, J. Appl. Cryst. 44 (2011) 1281–1284.
[22] S. Saeed, N. Rashid, P.G. Jones, M. Ali, R. Hussain, Eur. J. Med. Chem. 45 (2010) 1323–1331.
[23] C.H. Choi, M. Kertez, J. Phys. Chem. A 101 (1997) 3823–3831.
[24] M. Kurt, P. Chinna Babu, N. Sundaraganesan, M. Cinar, M. Karabacak, Spectrochim. Acta A 79 (2011) 1162–1170.
[25] D.F.V. Lewis, C. Ioannides, C.D.V. Xenobiotica 24 (1994) 401–408.
[26] L. Padmaja, R.C. Kunar, D. Sajan, I.H. Joe, V.S. Jayakunmar, G.R. Pettit, O.F. Nielsen, J. Raman Spectrosc. 40 (2009) 419–428.
[27] A. Poiyamozhi, N. Sundaraganesan, M. Karabacak, O. Tanriverdi, M. Kurt, J. Mol. Struc 1024 (2012) 1–12.
[28] P. Udhayakala, A. Jayanthi, T.V. Rajendiran, S. Gunasekaran, Arch. Appl. Sci. Res. 3 (2011) 424–439.
[29] R.G. Pearson, Proc. Natl. Acad. Sci. U. S. A. 83 (1986) 8440–8441.
[30] R.H. Chen, J.F. Xiang, P. Peng, G.Z. Mo, X.S. Tang, Z.Y. Wang, X.F. Wang, Asian J. Chem. 26 (2014) 926–932.
[31] P. Peng, J.F. Xiong, G.Z. Mo, J.L. Zheng, R.H. Chen, X.Y. Chen, Z.Y. Wang, Amino Acids (2014) 2427–2433.